

Locally preferred structures and many-body static correlations in viscous liquidsDaniele Coslovich^{1,2,*}¹*Laboratoire Charles Coulomb UMR 5221, Université Montpellier 2 and CNRS, Montpellier, France*²*Institut für Theoretische Physik and Center for Computational Materials Science, Technische Universität Wien, Vienna, Austria*

(Received 28 February 2011; published 16 May 2011)

The influence of static correlations beyond the pair level on the dynamics of selected model glass formers is investigated. The pair structure, angular distribution functions, and statistics of Voronoi polyhedra of two well-known Lennard-Jones mixtures as well as of the corresponding Weeks-Chandler-Andersen variants, in which the attractive part of the potential is truncated, are compared. By means of the Voronoi construction, the atomic arrangements corresponding to the locally preferred structures of the models are identified. It is found that the growth of domains formed by interconnected locally preferred structures signals the onset of the slow-dynamics regime and allows the rationalization of the different dynamic behaviors of the models. At low temperature, the spatial extension of the structurally correlated domains, evaluated at fixed relaxation time, increases with the fragility of the models and is systematically reduced by truncating the attractions. In view of these results, proper inclusion of many-body static correlations in theories of the glass transition appears crucial for the description of the dynamics of fragile glass formers.

DOI: [10.1103/PhysRevE.83.051505](https://doi.org/10.1103/PhysRevE.83.051505)

PACS number(s): 64.70.pm, 61.20.Ja, 64.70.qd

I. INTRODUCTION

The question of whether the structure of a glass differs from that of the corresponding liquid is often rhetorically posed within the glass community. In fact, very small differences are observed in the static structure factor of a viscous liquid as it approaches the glass transition temperature T_g . By contrast, the viscosity and structural relaxation times increase by several orders of magnitude upon supercooling and the motion of the molecules in the liquid becomes increasingly cooperative and spatially heterogeneous.

At first glance, the small structural changes discernible at the level of pair correlations appear insufficient to explain the dramatic slowing down of the liquid and the nontrivial spatial correlations of the dynamics. A preliminary indication that this may not necessarily be the case comes from the mode-coupling theory (MCT) of the glass transition [1]. The MCT predictions for the dynamic correlation functions are based uniquely on structural information, almost invariably the static structure factors of the liquid. Numerical solutions of the MCT equations for model liquids show that small variations of the pair-correlation functions, which develop upon lowering the temperature, can produce significant effects on the dynamics and eventually lead to an ergodic-nonergodic transition at some critical temperature T_{MCT} [2]. The generic predictions of the theory account rather well for experimental and numerical findings in weakly supercooled liquids [1,3] (i.e., for $T \geq T_{MCT}$). The breakdown of MCT at lower temperatures ($T_g < T \leq T_{MCT}$), where the actual system remains effectively ergodic, most likely reflects the mean-field character of the theory [4–6] and its inability to describe activated transitions between metastable glassy states [7]. Another delicate aspect that may affect the outcome of MCT is the exclusion of many-body correlations [8]. Three-body static correlations have been shown [9] to impact the MCT solutions for a model of silica [10], but not the ones for the

prototypical Kob-Andersen model [11]. Interestingly, a study of a schematic version of the generalized MCT [12–14], which allows proper description of many-body dynamic correlations, shows that the ideal transition at T_{MCT} can be delayed by retaining higher-order density correlations in the MCT equations [14].

The importance of high-order static correlations, hidden in the amorphous structure of the liquid, is particularly emphasized by frustration-based approaches to the glass transition [15–18]. According to these theories, the phenomenology of glass formation arises from the competition between the growth of slow, correlated domains, characterized by some preferred local order, and frustration, which prevents these domains from percolating through the liquid. Despite some disagreement on the interpretation of the role of frustration [19,20], these models indicate medium-range order and structural correlations beyond the pair level as key features for understanding the dynamic behavior of glass-forming systems.

Computer simulations of several model glassy systems [21–27] and experiments on dense colloidal suspensions [28,29] provide evidence for the existence of domains formed by preferred local structures and for their influence on the dynamics. Similar observations, albeit without explicit reference to the dynamics, emerge from recent *ab initio* simulations and experiments on metallic glasses [30,31]. Furthermore, high-order static correlations, named point-to-set correlations [32], have recently been revealed by simulations under amorphous boundary conditions and have been found to grow by decreasing temperature in a model supercooled liquid [33]. In spite of these advances, there is still no general consensus on the connection between the structure and dynamics in supercooled liquids. In particular, dynamic facilitation models [34] provide an alternative and physically appealing description of the glassy dynamics in terms of purely kinetic constraints.

A clear-cut procedure to test the influence of many-body static correlations on the dynamics of glass-forming liquids

*daniele.coslovich@univ-montp2.fr

emerges from recent work of Berthier and Tarjus [8,35]. These authors compared the pair structure and dynamics of two model glassy systems: the Kob-Andersen (KA) binary Lennard-Jones (LJ) mixture [11] and its Weeks-Chandler-Andersen (WCA) variant [36], in which the attractive part of the pair potential is truncated. Berthier and Tarjus found that, at fixed temperature and for sufficiently large density, the pair structure of the two models is almost identical, while the structural relaxation times can differ by orders of magnitude. Thus a direct comparison of the LJ and WCA models offers an ideal benchmark to test the existence and the influence of static correlations beyond the pair level. Building on prior knowledge of the preferred local order of LJ mixtures [26], here structural indicators of increasing complexity are considered—ranging from pair correlations, through angular distribution functions, to Voronoi tessellation—for selected LJ and WCA liquids and a crucial numerical experiment on the influence of the structure on the dynamics of the models is performed.

II. METHODS

Two well-known models of glass-forming liquids are considered: the Kob-Andersen binary mixture [11] and the Wahnström binary mixture (WAHN) [37]. In the original models [11,37], named herein KA-LJ and the WAHN-LJ models, particles interact through the LJ potential

$$u_{\alpha\beta}(r) = 4\epsilon_{\alpha\beta} \left[\left(\frac{\sigma_{\alpha\beta}}{r} \right)^{12} - \left(\frac{\sigma_{\alpha\beta}}{r} \right)^6 \right], \quad (1)$$

where $\alpha, \beta = 1, 2$ are species indices. The values of the parameters $\sigma_{\alpha\beta}$ and $\epsilon_{\alpha\beta}$ are $\sigma_{12} = 0.8\sigma_{11}$, $\sigma_{22} = 0.88\sigma_{11}$, $\epsilon_{12} = 1.5\epsilon_{11}$, and $\epsilon_{22} = 0.5\epsilon_{11}$ for the KA mixture and $\sigma_{12} = 0.916\sigma_{11}$, $\sigma_{22} = 0.833\sigma_{11}$, and $\epsilon_{22} = \epsilon_{12} = \epsilon_{11}$ for the WAHN mixture. The chemical compositions and mass ratios are $x_1 = 1 - x_2 = 0.8$ and $m_1/m_2 = 1$ (for the KA mixture) and $x_1 = x_2 = 0.5$ and $m_1/m_2 = 2$ (for the WAHN mixture). The potentials are cut and shifted by a quadratic term [38] at $2.5\sigma_{\alpha\beta}$ and $2.5\sigma_{11}$ in the KA and WAHN mixtures, respectively. In the following, σ_{11} , ϵ_{11} , and $\sqrt{m_1\sigma_{11}^2/\epsilon_{11}}$ are used as units of distance, energy, and time, respectively.

In addition, the corresponding WCA variants of the above mixtures are studied. In the WCA models [36,39], the interaction parameters $\sigma_{\alpha\beta}$ and $\epsilon_{\alpha\beta}$ and chemical compositions are unchanged, but each of the pair potentials $u_{\alpha\beta}(r)$ is truncated and shifted so that the value at the minimum is zero [39]. The WCA truncation of the attractive part of the potential is well known from liquid-state theories [39]. However, it was found in this work that this procedure leads to poor energy conservation during the long molecular dynamics simulations in the supercooled regime. To circumvent this problem, a smooth cutoff scheme with cubic interpolation [40] is employed to ensure continuity up to the second derivative of the potentials at the minimum $r_c = 2^{1/6}\sigma_{\alpha\beta}$ of the LJ potential. Explicitly, the WCA smooth (WCAS) potentials read

$$u_{\alpha\beta}^s(r) = \begin{cases} u_{\alpha\beta}(r) + A_{\alpha\beta}, & r < a_{\alpha\beta} \\ B_{\alpha\beta}(r_c - r)^3, & a_{\alpha\beta} < r < r_c \\ 0, & r > r_c, \end{cases} \quad (2)$$

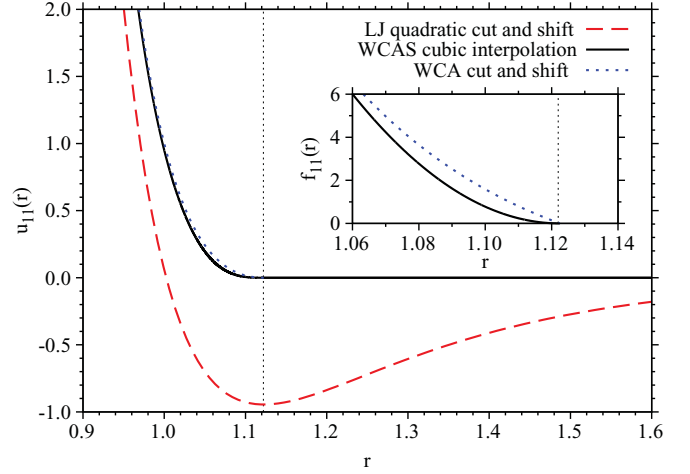


FIG. 1. (Color online) Pair potentials between particles of species 1 used in this study: LJ quadratic cut and shifted (dashed line), WCAS with cubic interpolation (solid line), and WCA cut and shifted (dotted line). Inset: Force between particles of species 1 for the WCAS (solid line) and the WCA (dotted line) potentials. In both panels, the dotted vertical line marks the distance $r = 2^{1/6}$ corresponding to the minimum of the LJ potential.

where $A_{\alpha\beta}$ and $B_{\alpha\beta}$ are determined to ensure continuity at $r = a$ and r_c . The parameters $a_{\alpha\beta}$ are adjusted for each pair α - β so that $r_c = 2^{1/6}\sigma_{\alpha\beta}$ and read $a_{11} = 1.0269$, $a_{12} = 0.8215$, and $a_{22} = 0.9038$ for the KA-WCAS mixture and $a_{11} = 1.0269$, $a_{12} = 0.9473$, and $a_{22} = 0.8555$ for the WAHN-WCAS mixture. A comparison between LJ, WCAS, and WCA potentials for 1-1 pairs is shown in Fig. 1. In contrast to the WCA potential, the derivative of the force of the WCASP is continuous at r_c . In the inset, the difference between the WCA and the WCAS potential in the $r \sim r_c$ region is highlighted. As it will be clear in the following, this modification introduces some small differences in the thermodynamic and dynamic properties, but does not qualitatively alter the comparison with LJ models. In the following, the focus will mostly be on the WCAS models and selected results will be reported for the original WCA models. All studied systems are composed of 1000 particles in a cubic box with periodic boundary conditions. Molecular dynamics simulations are performed in the NVT ensemble using the Nosé-Poincaré thermostat [41] with a mass parameter $Q = 5.0$. The number density of the KA mixtures is $\rho = 1.2$, while that of the WAHN mixtures is $\rho = 1.297$. For the LJ and WCAS models, static and dynamic properties are averaged over up to six independent thermal histories. The KA-WCAS mixture is found to crystallize more easily than the other systems [42]. A similar tendency to crystallize has been reported in Ref. [43] for the KA-WCA model. Only the noncrystallizing samples are retained to perform the averages.

III. RESULTS

A. Two-body and three-body static correlations

To start the discussion, the pair structure of the present models is analyzed. Figure 2 displays the radial distribution function $g_{12}(r)$ between unlike species in KA mixtures

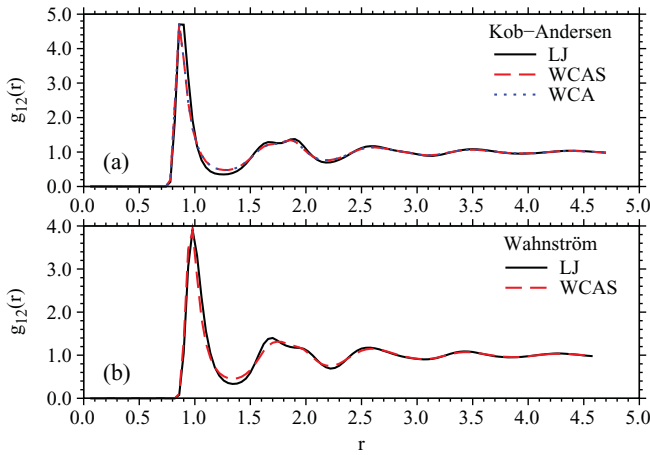


FIG. 2. (Color online) Radial distribution functions $g_{12}(r)$ for (a) the Kob-Andersen mixture and (b) the Wahnström mixtures. The state points considered are (a) $\rho = 1.2$, $T = 0.5$ and (b) $\rho = 1.297$, $T = 0.6$. In both panels, solid, dashed, and dotted lines indicate results for the LJ, WCAS, and WCA models, respectively. Error bars are smaller than the widths of the lines.

[Fig. 2(a)] and WAHN mixtures [Fig. 2(b)]. For each type of mixture, the results obtained are shown at a common temperature, representative of the slow-dynamics regime of the LJ models. The pair structure appears essentially unaffected by the truncation of attractions, thus confirming the observations of recent simulation works [8,44]. This result holds for both WCA and WCAS models. Only a close inspection of the figures reveals that the first minima of $g_{12}(r)$ are slightly deeper in the LJ models, suggesting that the latter systems are effectively more supercooled. A similar effect is visible in the radial distribution functions reported by Pedersen *et al.* [44] for KA-LJ and KA-WCA mixtures.

At the temperatures considered in Fig. 2, the structural relaxation times of the LJ and WCA models differ by almost two orders of magnitude, as is evident from Ref. [8] and Figs. 4 and 5 (discussed in further detail below). Given the small differences observed in the pair structure, it is natural to ask whether this large variation in the dynamic properties is due to the higher-order static correlations. In a first attempt to go beyond pair correlations, the bond-angle distribution functions $D_{\alpha\beta\gamma}(\theta)$ between triplets of neighboring particles of species α , β , and γ are calculated, where β is the species of the central particle. Figure 3 shows the angular distribution functions $D_{121}(\theta)$ for the same state points considered in Fig. 2. Angular correlations reveal more clearly the structural differences between the LJ and WCA models. In the KA mixtures, the sharp peaks in $D_{121}(\theta)$ around $\sim 70^\circ$ and the broad peak in the range 120° – 140° reflect local arrangements corresponding to distorted, twisted bicapped prisms of large particles (species 1) centered around small particles (species 2) [26]. A comparison of the LJ and WCA data sets thus reveals that the KA-LJ mixture has a more pronounced local ordering than the KA-WCA mixture at the selected thermodynamic state. As in the case of $g_{12}(r)$, the difference between the WCA and WCAS models is negligible for this state point. A similar effect is visible for the WAHN

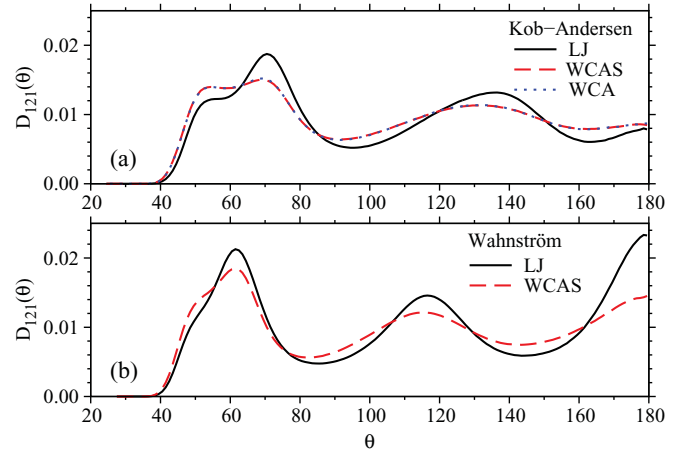


FIG. 3. (Color online) Angular distribution functions $D_{121}(r)$ for (a) Kob-Andersen mixtures and (b) Wahnström mixtures. State points and lines are the same as in Fig. 2. Error bars are smaller than the widths of the lines.

mixtures: The peaks in $D_{121}(\theta)$, located around 63° , 116° , and 180° , are signatures of local icosahedral ordering, which appears more pronounced in the original LJ model than in the WCAS variant. Similar conclusions can be drawn from an analysis of the other angular distribution functions (not shown here) and are corroborated by an inspection of data at even lower temperature. Thus the structures of the LJ and WCA systems differ more evidently at the level of three-body static

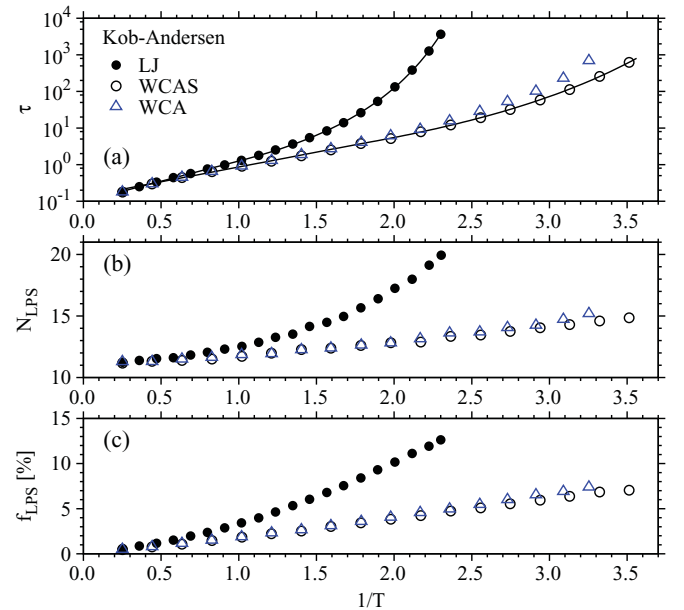


FIG. 4. (Color online) (a) Structural relaxation time τ as a function of $1/T$ for Kob-Andersen mixtures for the LJ (filled circles), WCAS (open circles), and WCA (open triangles) models. The wave vector considered for the calculation of τ is $k = 7.0$. Fits to the modified Vogel-Fulcher-Tammann equation [Eq. (3)] are shown as solid lines. (b) Average number N_{LPS} of particles in locally preferred structure (LPS) domains formed by (0,2,8) polyhedra. Symbols have the same meaning as in (a). (c) Average fraction of particles of species 2 at the center of (0,2,8) polyhedra as a function of $1/T$. Symbols have the same meaning as in (a).

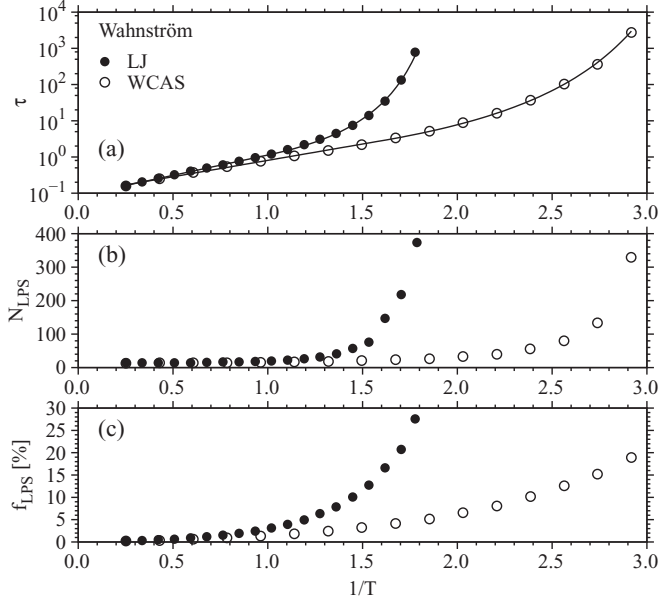


FIG. 5. Same as Fig. 4 but for Wahnström mixtures. For these systems, the LPS corresponds to (0,0,12) polyhedra.

correlations and the increase of local ordering upon switching on attractions correlates qualitatively with the increase of relaxation times.

B. Locally preferred structures

To render the connection between the local structure and dynamics explicit, the statistics of Voronoi polyhedra are

analyzed as a function of temperature. The Voronoi tessellation implicitly entails more complex static correlations (although, of course, it cannot be expressed as a multiparticle correlation function) and reveals the details of the particles' arrangements within the first coordination shell. Inspection of the spatial persistence of a given local structure provides information on extended structural correlations, i.e., medium-range order. The protocol adopted here is the same as that used in a prior investigation of the local structure of binary LJ mixtures at constant pressure [26]. The temperature dependence of the fraction of Voronoi polyhedra with a given signature (n_3, n_4, \dots) is monitored, where n_i is the number of faces of the polyhedron with a given number i of vertices. The locally preferred structure (LPS) of the liquid is identified as the geometrical arrangement corresponding to the most frequent Voronoi polyhedron around particles of species 2 observed in the samples at low temperature. This choice is based on the observation that in binary LJ mixtures it is easier to characterize local order around small particles [26,45]. This is also consistent with a previous study of the KA-LJ mixture, which focused on the coordination polyhedra of large particles around the small ones [46]. The most frequent signatures of Voronoi polyhedra around particles of species 2 and 1 are reported in Tables I and II, respectively. It is found herein that the typical Voronoi polyhedra observed around particles of species 1 [such as (0,2,8,4) or (0,1,10,4) polyhedra] do not display evident symmetries and lack a clear structural identification. Furthermore, the corresponding percentages do not increase as sharply upon decreasing temperature as those calculated for Voronoi polyhedra around particles of species 2. In the following, the analysis will therefore be

TABLE I. Most frequent signatures of Voronoi polyhedra around particles of species 2 from instantaneous configurations and local minima of the potential energy surface. Percentages are calculated with respect to the number of particles of species 2. The low-temperature data set ($T = T_l$) corresponds to the lowest available temperatures: $T = 0.435$ (for KA-LJ mixture), $T = 0.285$ (for KA-WCAS mixture), $T = 0.560$ (for the WAHN-LJ mixture), and $T = 0.343$ (for the WAHN-WCAS mixture). The high-temperature data set ($T \approx T^*$) corresponds to temperatures close to the crossover temperature T^* : $T = 0.983$ (KA-LJ), $T = 0.627$ (KA-WCAS), $T = 1.072$ (WAHN-LJ), and $T = 0.598$ (WAHN-WCAS).

Mixture	Instantaneous configurations				Local minima			
	$T = T_l$		$T \approx T^*$		$T = T_l$		$T \approx T^*$	
	%	Signature	%	Signature	%	Signature	%	Signature
KA-LJ	12.6	(0,2,8)	4.0	(0,2,8,1)	19.9	(0,2,8)	12.4	(0,2,8)
	8.3	(1,2,5,3)	3.9	(1,2,5,3)	7.2	(1,2,5,3)	5.9	(1,2,5,3)
	5.6	(1,2,5,2)	3.4	(0,2,8)	6.8	(1,2,5,2)	5.8	(1,2,5,2)
	5.1	(0,3,6)	3.2	(0,4,4,3)	6.7	(0,3,6)	5.3	(0,3,6,1)
KA-WCAS	7.1	(0,2,8)	3.9	(0,2,8,1)	8.4	(0,2,8)	5.2	(0,2,8)
	5.7	(1,2,5,3)	3.5	(1,2,5,3)	5.4	(1,2,5,3)	4.1	(1,2,5,3)
	4.7	(0,2,8,1)	3.4	(0,3,6,3)	4.5	(1,2,5,2)	4.0	(0,4,4,3)
	3.7	(0,4,4,3)	3.1	(0,4,4,3)	4.3	(0,2,8,1)	3.9	(1,2,5,2)
WAHN	27.4	(0,0,12)	7.0	(0,3,6,4)	32.7	(0,0,12)	10.9	(0,0,12)
	9.0	(0,2,8,2)	5.2	(0,2,8,2)	10.0	(0,2,8,2)	10.6	(0,2,8,2)
	7.7	(0,1,10,2)	3.5	(0,1,10,2)	8.3	(0,1,10,2)	9.7	(0,3,6,4)
	6.0	(0,3,6,4)	3.0	(0,3,6,3)	6.5	(0,3,6,4)	7.3	(0,1,10,2)
WAHN-WCAS	18.9	(0,0,12)	7.7	(0,3,6,4)	20.0	(0,0,12)	8.5	(0,3,6,4)
	9.1	(0,2,8,2)	6.4	(0,2,8,2)	9.8	(0,2,8,2)	7.9	(0,2,8,2)
	7.2	(0,3,6,4)	4.3	(0,1,10,2)	7.4	(0,3,6,4)	5.8	(0,0,12)
	6.9	(0,1,10,2)	4.1	(0,0,12)	6.6	(0,1,10,2)	4.7	(0,1,10,2)

TABLE II. Same as Table I but for Voronoi polyhedra around particles of species 1. Percentages are calculated with respect to the number of particles of species 1.

Mixture	Instantaneous configurations				Local minima			
	$T = T_l$		$T \approx T^*$		$T = T_l$		$T \approx T^*$	
	%	Signature	%	Signature	%	Signature	%	Signature
KA-LJ	7.8	(0,2,8,4)	4.7	(0,2,8,4)	8.7	(0,2,8,4)	7.2	(0,2,8,4)
	5.7	(0,2,8,5)	3.2	(0,3,6,5)	6.6	(0,2,8,5)	5.1	(0,2,8,5)
	5.0	(0,3,6,6)	3.0	(0,3,6,4)	5.3	(0,3,6,6)	4.1	(0,3,6,6)
	4.4	(0,3,6,5)	2.9	(0,2,8,5)	4.8	(0,1,10,4)	4.1	(0,1,10,2)
KA-WCAS	7.4	(0,2,8,4)	5.2	(0,2,8,4)	7.5	(0,2,8,4)	6.1	(0,2,8,4)
	5.0	(0,2,8,5)	3.5	(0,3,6,5)	5.1	(0,2,8,5)	3.9	(0,2,8,5)
	4.7	(0,3,6,6)	3.2	(0,3,6,4)	4.9	(0,3,6,6)	3.8	(0,3,6,5)
	4.5	(0,3,6,5)	3.2	(0,3,6,6)	4.4	(0,3,6,5)	3.8	(0,3,6,6)
WAHN	8.0	(0,1,10,4)	4.7	(0,2,8,4)	9.5	(0,1,10,4)	7.4	(0,2,8,5)
	7.1	(0,2,8,5)	3.7	(0,2,8,5)	8.5	(0,2,8,5)	6.8	(0,2,8,4)
	6.3	(0,2,8,4)	3.2	(0,3,6,6)	6.7	(0,2,8,4)	5.4	(0,1,10,4)
	4.7	(0,1,10,3)	3.0	(0,3,6,5)	5.2	(0,1,10,3)	4.6	(0,3,6,6)
WAHN-WCAS	7.6	(0,2,8,5)	5.8	(0,2,8,4)	8.0	(0,2,8,5)	6.3	(0,2,8,4)
	6.9	(0,2,8,4)	4.8	(0,2,8,5)	6.9	(0,2,8,4)	5.8	(0,2,8,5)
	6.8	(0,1,10,4)	3.8	(0,3,6,6)	6.8	(0,1,10,4)	4.4	(0,3,6,6)
	4.6	(0,1,10,3)	3.4	(0,3,6,5)	4.5	(0,1,10,3)	3.6	(0,1,10,4)

based on the local structures observed around this latter type of particle. Understanding the nature of local order around large particles remains an open issue, which may need more refined methods to detect short- and medium-range order.

The present results confirm the observations of Ref. [26] at constant pressure: In the low-temperature regime, (0,2,8) and (0,0,12) polyhedra around particles of species 2 constitute the dominant signatures in KA-LJ and WAHN-LJ mixtures, respectively. Thus the LPSs of the KA-LJ and WAHN-LJ mixtures are identified as twisted bicapped square prisms and icosahedra, respectively [26]. The identification is consistent with previous investigations on KA-LJ clusters [47] and with a recent simulation study on the bulk WAHN-LJ mixture [48]. By applying the same procedure to the WCA and WCAS models, the locally preferred structures are found to remain the same as in the original LJ models. However, a systematic reduction of the fraction of LPSs upon truncating the attractions is observed. This effect will be discussed in further detail below.

As a general rule, the fraction f_{LPS} of particles of species 2 at the center of a LPS increases with decreasing temperature [26]. The growth of f_{LPS} reflects the formation of slow, long-lived clusters of neighboring LPSs [26]. A calculation of the self-intermediate scattering functions filtered according to the pertinent Voronoi polyhedra shows that the typical relaxation times of particles at the center of LPSs are up to 10 times larger than those outside LPSs [26]. In the following, these clusters will be referred to as LPS domains, which are defined as groups of particles sitting either at the center or on the vertices of face-sharing polyhedra with the signature of the LPS. The average number of particles forming a LPS domain will be denoted by N_{LPS} , which is a measure of the spatial extension over which the liquid adopts the same preferred local structure [49]. In Figs. 4(b) and 5(b) N_{LPS} is shown as a function of $1/T$

for the the KA and WAHN models, respectively. To facilitate the comparison with previous work [26], the temperature dependence of f_{LPS} is included in Figs. 4(c) and 5(c). Note that, while f_{LPS} is evaluated with respect to particles of species 2, both species of particles contribute to the size N_{LPS} of LPS domains. Both N_{LPS} and f_{LPS} increase in a similar fashion as T decreases, although with slightly different functional forms. The growth of LPS domains is particularly dramatic in Wahnström mixtures, which develop a strong icosahedral order upon supercooling. By contrast, the size of the domains formed by prismatic structures in KA models is relatively small (20–30 particles). Nonetheless, the structural evolution in all the systems studied follow qualitatively similar patterns.

C. Connection between structure and dynamics

To illustrate the connection to the dynamics of the models, WCAS the temperature dependence of the structural relaxation times τ is studied. The latter are defined by the condition $F_s(k = 7, \tau) = 1/e$, where $F_s(k, t)$ is the self-intermediate scattering function averaged over all particles. The relaxation times have been fitted by the following modified Vogel-Fulcher-Tammann (VFT) equation [26]:

$$\tau(T) = \begin{cases} \tau_\infty \exp(E_\infty/T), & T > T^* \\ \tau'_\infty \exp\left(\frac{1}{K(T/T_0 - 1)}\right), & T < T^*, \end{cases} \quad (3)$$

where

$$\tau'_\infty = \tau_\infty \exp\left(E_\infty/T^* - \frac{1}{K(T^*/T_0 - 1)}\right). \quad (4)$$

Equation (3) ensures a smooth crossover around T^* between the Arrhenius law at high T and the VFT equation at low

T , accounting for the super-Arrhenius dependence of the relaxation times. Figures 4(a) and 5(a) display τ as a function of $1/T$ for the KA and WAHN mixtures, respectively, together with the corresponding fits to Eq. (3). Figure 4(a) also includes results for the KA-WCA mixture obtained using the original cut and shift at the minimum of the potentials, as in previous works [8,35,36]. The latter data set is in good agreement with the results obtained in Refs. [8,35] for a similar wave vector ($k = 7.21$). At sufficiently low temperature, however, non-negligible deviations appear with respect to the KA-WCAS mixture. This discrepancy may be attributed to the modification induced by the smooth cutoff employed in this work. The comparison between the LJ and WCAS models, however, remains qualitatively unaffected and confirms the general conclusions of Refs. [8,35].

A comparison of the LPS analysis and relaxation times data reveals a striking relationship between structure and dynamics. The increase of τ below the crossover temperature T^* correlates to the increase in size of the LPS domains. This connection is particularly evident for the two WAHN mixtures, in which the increase of icosahedral order upon decreasing T is very sharp. The results herein reveal that the large difference in the dynamic behavior between the LJ and WCA models reflects different stages of the evolution of the local structure on the way to glass formation—an effect that is barely visible at the level of pair correlations. It should be noted that the size of the LPS domains at low temperature is slightly larger in the WCA model than in the WCAS model, which is consistent with the discrepancy in relaxation times observed above.

A remark on the nature of local order in these models is in order. It has been shown recently that the WAHN-LJ mixture can phase separate and then partially crystallize in a complex crystal structure that accommodates distorted icosahedral geometries [48]. The LPS observed in the liquid is thus analogous to the typical local structure of the underlying crystal, which is at odds with the paradigm of the frustration-limited domains theory [16]. The situation is less clear in the case of the KA-LJ mixture, for which an unambiguous identification of the crystalline phase is lacking. Previous studies [50,51] have shown that, for chemical compositions close to the one of the original model, stable crystals either have CsCl symmetry or are composed of a mixture of fcc and hcp structures of large particles. Interestingly, in the present work it was found that the KA-WCAS model can crystallize into a fcc lattice of large particles. In this model crystallization is associated with a sudden drop in the fraction of (0,2,8) polyhedra and a rapid increase in (0,4,4,6) polyhedra centered around particles of species 1. This reveals a potential mismatch between the LPS of the liquid and the typical local structure of the crystal. The question of whether the locally preferred structure should be different from the structure of the underlying crystal [19,20] certainly deserves further investigation.

D. Connections between structure, potential-energy landscape, and fragility

The connection between the growth of LPS domains and slow dynamics is further corroborated by the analysis of the potential energy landscape (PEL). It is well known that the

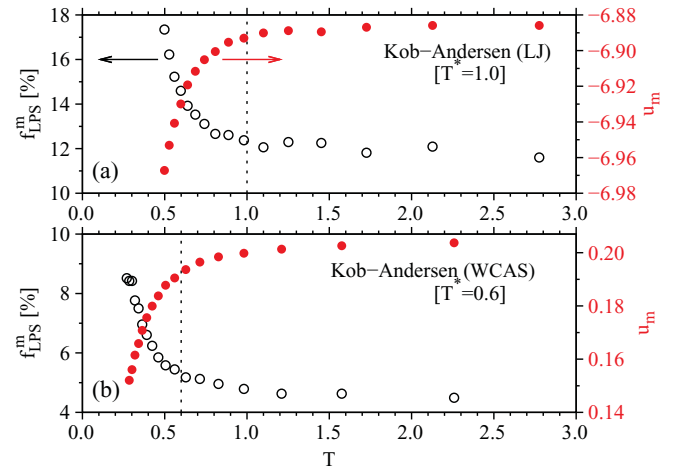


FIG. 6. (Color online) Average fraction f_{LPS}^m of LPSs in local minima (open circles, left axis) and average potential energy u_m of local minima (filled circles, right axis) as a function of T for Kob-Andersen mixtures for (a) the LJ model and (b) the WCAS model. The dynamic crossover temperatures T^* obtained from fits to Eq. (3) are indicated as vertical dotted lines.

appearance of super-Arrhenius behavior and nonexponential relaxation around the so-called onset temperature T_O coincides with a sharp change in the properties of the local minima of the PEL explored by system [52]. In fact, the average energy $u_m(T)$ of local minima remains almost constant at high T and starts decreasing rapidly below T_O . Figures 6 and 7 display u_m and the fraction f_{LPS}^m of particles of species 2 at the center of the LPSs evaluated for local minima of the PEL as a function of temperature for the KA and WAHN mixtures, respectively. We note that the values of T^* obtained from Eq. (3) are only slightly larger than the onset temperatures estimated from the appearance of two-step, nonexponential relaxation in the dynamic correlation functions and are consistent, at least for KA mixtures, with the values of T_O reported in Ref. [53].

Strikingly, the onset of slow dynamics, indicated by the drop in u_m , always correlates to a sharp increase in f_{LPS}^m . It

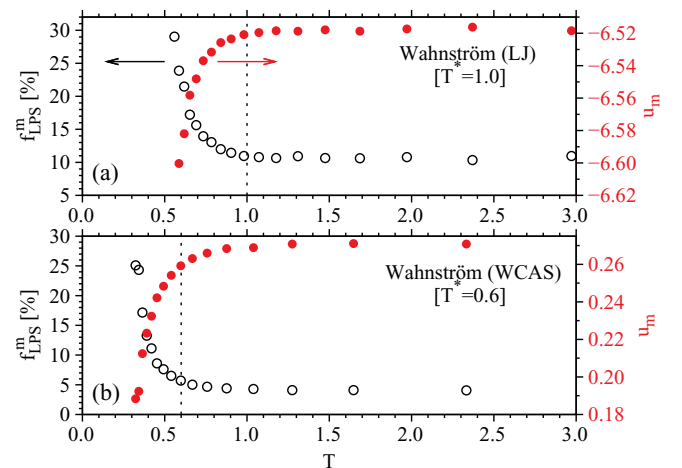


FIG. 7. (Color online) Same as Fig. 6 but for Wahnström mixtures. The vertical axes are analogous to those in Fig. 6.

should be noted that the percentages of other less frequent signatures of Voronoi polyhedra do not increase as sharply across T^* , although some of them do display some change upon decreasing T (see Table I). The onset of slow dynamics in the models studied herein is thus attributed to the growth of structural correlations. It should also be noted that landscape approaches based on high-order stationary points of the potential-energy surface [40] may provide results that are complementary to those in the present work. In fact, it was found that particles at the center of LPSs participate less to unstable modes of saddle points [54–56]. Establishing a clear relationship between the growth of LPSs and the disappearance of unstable directions in the landscape is an interesting open issue that is left for future investigation.

The present findings ostensibly indicate that the drop in u_m is connected to the formation of energetically favored structures. This is consistent with the observation that the potential energy associated with the LPS is typically lower than that of other structures [54]. In general, however, specific local structures may be favored also for nonenergetic reasons, such as more efficient packing or nontrivial entropic effects (e.g., favorable arrangements of interlocking LPSs). An interesting example of this competition is provided by a model of a NiY alloy based on LJ interactions [45], for which the LPS—a capped trigonal prismatic structure—corresponds to a Voronoi polyhedron having the smallest volume but not the lowest potential energy [54]. Different groups have attempted to account for this complex interplay at the mean-field level in the one-component LJ liquid [57] and in a soft-sphere mixture [58,59]. It would be interesting to use these approaches for the systems studied herein.

To set forth the present results in a more compact fashion, τ is plotted as a function of N_{LPS} (see Fig. 8), thereby making the temperature dependence implicit. This representation of the data allows several system-specific aspects of the relationship between the structure and dynamics to be illustrated more clearly. As expected, it is found that the increase of τ correlates to that of N_{LPS} . However, the spatial extension of LPS domains

at fixed relaxation times increases systematically with the fragility K of the model, which is estimated from fitting the relaxation times to Eq. (3). In the case of the more fragile WAHN mixtures, the increase of relaxation times is evidently dictated by the growth of LPS domains. Over the same range of τ , the less fragile KA mixtures show a weaker structural change, indicating that other effects, such as dynamic facilitation, may also be playing an important role. The overall trend of variation is consistent with the correlation between the fragility and thermal rate of growth of LPSs put forth in Ref. [26] and suggests that the impact of static correlations on the dynamics should be more pronounced the more fragile the liquid. It should also be noted that the inclusion of attractions tends to increase N_{LPS} at fixed relaxation times. This stabilization effect is in qualitative agreement with recent observations on LJ and WCA fluids close to the triple point [60].

IV. CONCLUSION

A crucial test on the dynamic role of static correlations in glass-forming liquids has been performed by comparing two well-studied LJ mixtures and their corresponding purely repulsive variants. Truncation of the attractive part of the potential considerably shifts the glass transition to lower temperatures and reduces the fragility of the liquid, but does not alter the pair structure significantly [35]. These phenomena have been explained by resorting to indicators revealing more complex structural correlations. Building on prior work [26], correlated domains formed by locally preferred structures have been identified. It was found that the growth, by decreasing the temperature, of LPS domains is tightly connected to the onset of the slow-dynamics regime. Furthermore, an analysis of LPS domains has allowed the different dynamic behaviors of the LJ and WCAS models to be clearly distinguished in terms of their structure. In retrospect, these results suggest that even small differences that are discernible at the level of pair correlations may reflect substantially different stages of the structural evolution of a supercooled liquid and be associated with very different dynamic regimes. A solution of the MCT equations for the dynamic correlation functions—using two-body static correlations as input—only partially accounts for the different dynamic behaviors of the LJ and WCA models [8,61]. Thus, proper inclusion of many-body static correlations in theories of the glass transition based on structural information seems crucial for a correct description of the dynamics in fragile glass formers. This suggests revisiting and extending previous attempts [9] along these lines based on mode-coupling theory. Investigations of high-order static correlations extracted from simulations under amorphous boundary conditions [33], using patch repetition [62] or order mining methods [63], as well as implementation of alternative methods for LPS determination [28,64], may provide further clues to improve our theoretical understanding of the glass transition.

ACKNOWLEDGMENTS

Useful discussions with L. Berthier, W. Kob, and G. Pastore are acknowledged. The author acknowledges partial financial support by the Austrian Science Fund FWF under Project No. P19890-N16.

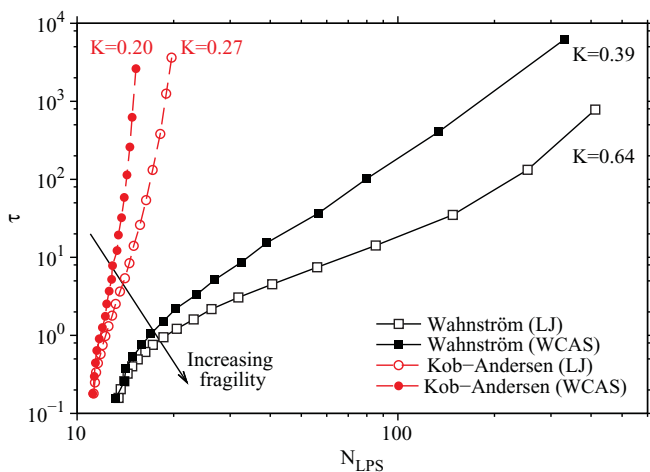


FIG. 8. (Color online) Relaxation time τ as a function of the average number N_{LPS} of particles in the LPS domains. The corresponding fragility indices K of the models, obtained from fits to the modified VFT equation [Eq. (3)], are also indicated.

- [1] W. Götze, *J. Phys. Condens. Matter* **11**, A1 (1999).
- [2] M. Nauroth and W. Kob, *Phys. Rev. E* **55**, 657 (1997).
- [3] S. P. Das, *Rev. Mod. Phys.* **76**, 785 (2004).
- [4] Y. Brumer and D. R. Reichman, *Phys. Rev. E* **69**, 041202 (2004).
- [5] A. Andreanov, G. Biroli, and J.-P. Bouchaud, *Europhys. Lett.* **88**, 16001 (2009).
- [6] A. Ikeda and K. Miyazaki, *Phys. Rev. Lett.* **104**, 255704 (2010).
- [7] V. Lubchenko and P. G. Wolynes, *Annu. Rev. Phys. Chem.* **58**, 235 (2007).
- [8] L. Berthier and G. Tarjus, *Phys. Rev. E* **82**, 031502 (2010).
- [9] W. Kob, M. Nauroth, and F. Sciortino, *J. Non-Cryst. Solids* **307**, 181 (2002).
- [10] B. W. H. van Beest, G. J. Kramer, and R. A. van Santen, *Phys. Rev. Lett.* **64**, 1955 (1990).
- [11] W. Kob and H. C. Andersen, *Phys. Rev. E* **51**, 4626 (1995).
- [12] G. Szamel, *Phys. Rev. Lett.* **90**, 228301 (2003).
- [13] J. Wu and J. Cao, *Phys. Rev. Lett.* **95**, 078301 (2005).
- [14] P. Mayer, K. Miyazaki, and D. R. Reichman, *Phys. Rev. Lett.* **97**, 095702 (2006).
- [15] D. Kivelson, S. A. Kivelson, X. Zhao, Z. Nussinov, and G. Tarjus, *Physica A* **219**, 27 (1995).
- [16] G. Tarjus, D. Kivelson, and P. Viot, *J. Phys. Condens. Matter* **12**, 6497 (2000).
- [17] H. Tanaka, *J. Non-Cryst. Solids* **351**, 3371 (2005).
- [18] H. Tanaka, *J. Non-Cryst. Solids* **351**, 3385 (2005).
- [19] F. Sausset and G. Tarjus, *Phys. Rev. Lett.* **100**, 099601 (2008).
- [20] T. Kawasaki, T. Araki, and H. Tanaka, *Phys. Rev. Lett.* **100**, 099602 (2008).
- [21] T. Tomida and T. Egami, *Phys. Rev. B* **52**, 3290 (1995).
- [22] M. Dzugutov, S. I. Simdyankin, and F. H. M. Zetterling, *Phys. Rev. Lett.* **89**, 195701 (2002).
- [23] T. S. Jain and J. de Pablo, *J. Chem. Phys.* **122**, 174515 (2005).
- [24] H. Shintani and H. Tanaka, *Nature Phys.* **2**, 200 (2006).
- [25] I. Ladadwa and H. Teichler, *Phys. Rev. E* **73**, 031501 (2006).
- [26] D. Coslovich and G. Pastore, *J. Chem. Phys.* **127**, 124504 (2007).
- [27] F. Sausset and G. Tarjus, *Phys. Rev. Lett.* **104**, 065701 (2010).
- [28] C. P. Royall, S. R. Williams, T. Ohtsuka, and H. Tanaka, *Nature Mater.* **7**, 556 (2008).
- [29] H. Tanaka, T. Kawasaki, H. Shintani, and K. Watanabe, *Nature Mater.* **9**, 324 (2010).
- [30] T. Fujita, K. Konno, W. Zhang, V. Kumar, M. Matsuura, A. Inoue, T. Sakurai, and M. W. Chen, *Phys. Rev. Lett.* **103**, 075502 (2009).
- [31] A. Hirata, P. Guan, T. Fujita, Y. Hirotsu, A. Inoue, A. R. Yavari, T. Sakurai, and M. Chen, *Nature Mater.* **10**, 28 (2011).
- [32] A. Montanari and G. Semerjian, *J. Stat. Phys.* **125**, 23 (2006).
- [33] G. Biroli, J.-P. Bouchaud, A. Cavagna, T. S. Grigera, and P. Verrocchio, *Nature Phys.* **4**, 771 (2008).
- [34] J. P. Garrahan and D. Chandler, *Proc. Natl. Acad. Sci. USA* **100**, 9710 (2003).
- [35] L. Berthier and G. Tarjus, *Phys. Rev. Lett.* **103**, 170601 (2009).
- [36] D. Chandler, J. P. Garrahan, R. L. Jack, L. Maibaum, and A. C. Pan, *Phys. Rev. E* **74**, 051501 (2006).
- [37] G. Wahnström, *Phys. Rev. A* **44**, 3752 (1991).
- [38] S. D. Stoddard and J. Ford, *Phys. Rev. A* **8**, 1504 (1973).
- [39] J. D. Weeks, D. Chandler, and H. C. Andersen, *J. Chem. Phys.* **54**, 5237 (1971).
- [40] T. S. Grigera, A. Cavagna, I. Giardina, and G. Parisi, *Phys. Rev. Lett.* **88**, 055502 (2002).
- [41] S. Nosé, *J. Phys. Soc. Jpn.* **70**, 75 (2001).
- [42] In this case, four samples out six crystallized around $T \sim 0.3$.
- [43] S. Toxvaerd, U. R. Pedersen, T. B. Schröder, and J. C. Dyre, *J. Chem. Phys.* **130**, 224501 (2009).
- [44] U. R. Pedersen, T. B. Schröder, and J. C. Dyre, *Phys. Rev. Lett.* **105**, 157801 (2010).
- [45] R. G. Della Valle, D. Gazzillo, R. Frattini, and G. Pastore, *Phys. Rev. B* **49**, 12625 (1994).
- [46] J. R. Fernández and P. Harrowell, *J. Phys. Chem. B* **108**, 6850 (2004).
- [47] J. P. K. Doye, A. A. Louis, I.-C. Lin, L. R. Allen, E. G. Noya, A. W. Wilber, H. C. Kok, and R. Lyus, *Phys. Chem. Chem. Phys.* **9**, 2197 (2007).
- [48] U. R. Pedersen, T. B. Schröder, J. C. Dyre, and P. Harrowell, *Phys. Rev. Lett.* **104**, 105701 (2010).
- [49] Note that this correlation does not require neighboring LPSs to be oriented in a similar fashion, provided a preferred direction of the LPSs could be defined.
- [50] J. R. Fernández and P. Harrowell, *J. Phys. Chem. B* **108**, 6850 (2004).
- [51] L.-C. Valdes, F. Affouard, M. Descamps, and J. Habasaki, *J. Chem. Phys.* **130**, 154505 (2009).
- [52] S. Sastry, P. G. Debenedetti, and F. H. Stillinger, *Nature (London)* **393**, 554 (1998).
- [53] Y. S. Elmatad, D. Chandler, and J. P. Garrahan, *J. Phys. Chem. B* **114**, 17113 (2010).
- [54] D. Coslovich, Ph.D. thesis, Università degli Studi di Trieste, 2008.
- [55] D. Coslovich and G. Pastore, *J. Chem. Phys.* **127**, 124505 (2007).
- [56] D. Coslovich (unpublished).
- [57] S. Mossa and G. Tarjus, *J. Chem. Phys.* **119**, 8069 (2003).
- [58] H. G. E. Hentschel, V. Ilyin, N. Makedonska, I. Procaccia, and N. Schupper, *Phys. Rev. E* **75**, 050404(R) (2007).
- [59] E. Lerner, I. Procaccia, and J. Zylberg, *Phys. Rev. Lett.* **102**, 125701 (2009).
- [60] J. Taffs, A. Malins, S. R. Williams, and C. P. Royall, *J. Chem. Phys.* **133**, 244901 (2010).
- [61] T. Voigtmann, *Phys. Rev. Lett.* **101**, 095701 (2008).
- [62] J. Kurchan and D. Levine, *J. Phys. A* **44**, 035001 (2011).
- [63] X. W. Fang, C. Z. Wang, Y. X. Yao, Z. J. Ding, and K. M. Ho, *Phys. Rev. B* **82**, 184204 (2010).
- [64] S. Mossa and G. Tarjus, *J. Non-Cryst. Solids* **352**, 4847 (2006).